

**Supplementary information:**

**Ca-oxalate crystals are involved in cadmium storage in a high Cd accumulating cultivar of cacao**

Hester Blommaert<sup>a\*</sup>, Hiram Castillo-Michel<sup>b</sup>, Giulia Veronesi<sup>c</sup>, Rémi Tucoulou<sup>b</sup>, Jacques Beauchêne<sup>d</sup>, Pathmanathan Umaharan<sup>e</sup>, Erik Smolders<sup>f</sup>, Géraldine Sarret<sup>a\*</sup>

<sup>a</sup>Université Grenoble Alpes, Université Savoie Mont Blanc, CNRS, IRD, Université G. Eiffel, ISTerre, Grenoble, France

<sup>b</sup>ESRF, The European Synchrotron, CS 40220, 38043 Grenoble Cedex 9, France

<sup>c</sup>Université Grenoble Alpes, CNRS, CEA, IRIG, Laboratoire de Chimie et Biologie des Métaux, 17 rue des Martyrs, 38000 Grenoble, France

<sup>d</sup>CIRAD, UMR Ecologie des Forêts de Guyane (EcoFoG), AgroParisTech, CNRS, INRA, Université des Antilles, Université de Guyane, 97310, Kourou, France

<sup>e</sup>Cocoa Research Centre, University of the West Indies, St. Augustine, Trinidad and Tobago

<sup>f</sup>Division of Soil and Water Management, Department of Earth and Environmental Sciences, KU Leuven, Belgium

### **1.1. Procedure to build Cd $\mu$ XRF maps**

In a normal procedure, a batch fitting file is created which attributes each XRF peak to an element based on its respective emission lines and defines the corresponding ROIs (Castillo-michel et al., 2017). However, the batch fitting routine with the model implemented in the PyMCA software, was not able to fit two background contributions, which were attributed to the sample matrix and to the K inelastic scattering. As a consequence, the batch fitting file was not able to fit the Cd peak well (at 3537.6 eV). On the one hand, in the Sr-hotspots there was a contribution on the left side of the peak which was originating from background scatter (related to the matrix of the Ca-crystals) (Figure S2 A). On the other hand, in the vessel structures, there was a contribution on the right side of the peak originating from K inelastic scatter (Figure S2 B). To extract only the Cd peak, we defined manually three gaussians (Figure S3). The first gaussian represents the background scatter from the crystals. The second gaussian is the real Cd signal and the third gaussian is the inelastic scatter. By fitting the three gaussians manually, we could extract the second gaussian and build the Cd XRF maps with this peak.

## 1.2. Supplementary figures

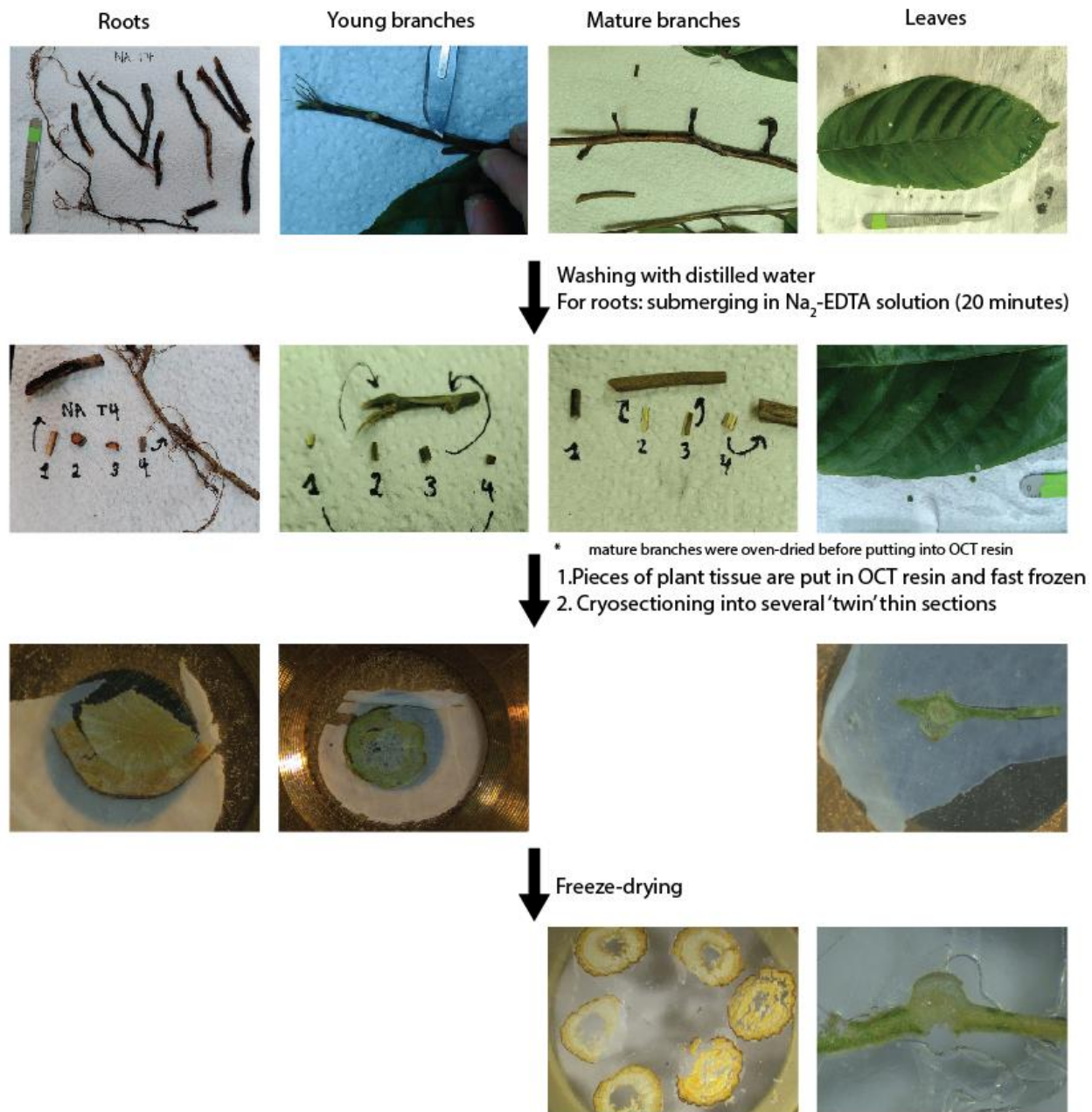


**Figure S1:** Scheme of sample preparation steps for  $\mu$ XRF (roots, young branches, and leaves) and nXRF analyses (mature branches, leaves) (Table 1).

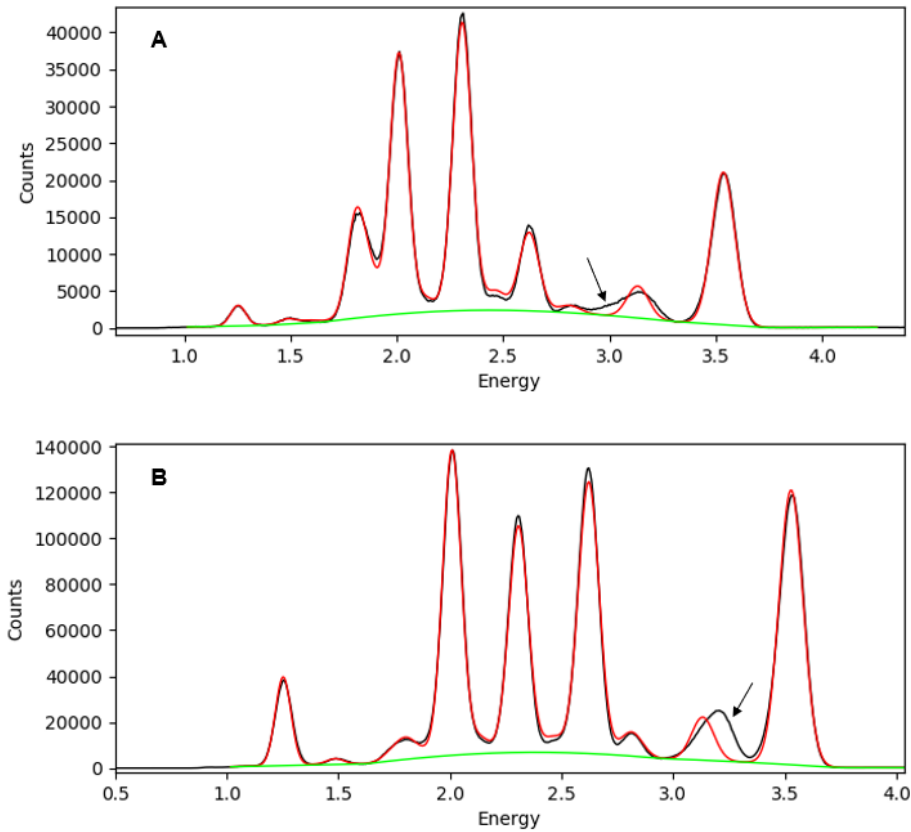


**Figure S2:** Example of XRF spectra. A) There is a background contribution (indicated with the arrow) which overlaps with the Cd emission line which is probably originating from the Ca crystals. B) There is a background contribution from the inelastic scattering of K.

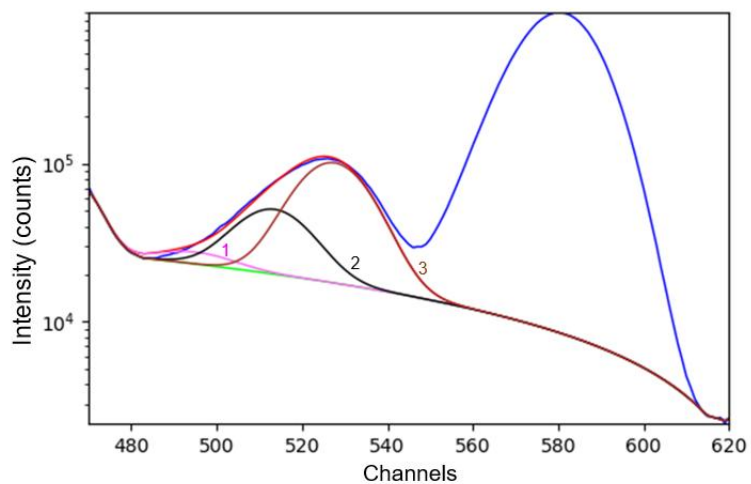


**Figure S3:** The three different gaussians defined. Gaussian 1 is the background originating from Ca crystals, gaussian 2 is the Cd peak, gaussian 3 is the contribution from K inelastic scattering. The Cd peak (2) was used to build the Cd XRF maps.

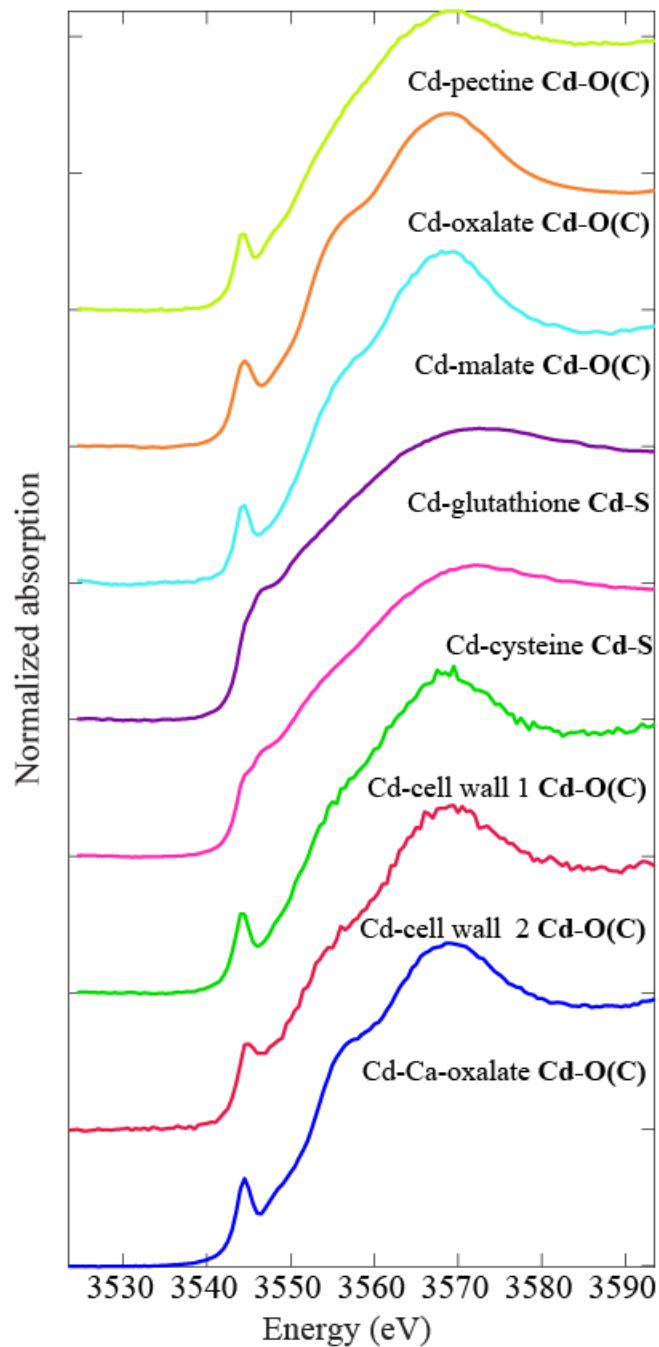


**Figure S4:** Cd L<sub>III</sub>-edge XANES spectra of selected reference materials. A database of Cd reference spectra recorded previously (Isaure et al., 2006) containing Cd-O species (Cd-cell wall, Cd-malate, Cd-oxalate, and Cd-pectin), and Cd-S species (Cd-cysteine and Cd-glutathione) was used for linear combination fitting. Cd-cell wall was remeasured during the measurement to

calibrate the samples on the previously recorded database. As additional standard, Cd-Ca-Oxalate (Cd-O) was measured and included in the database.

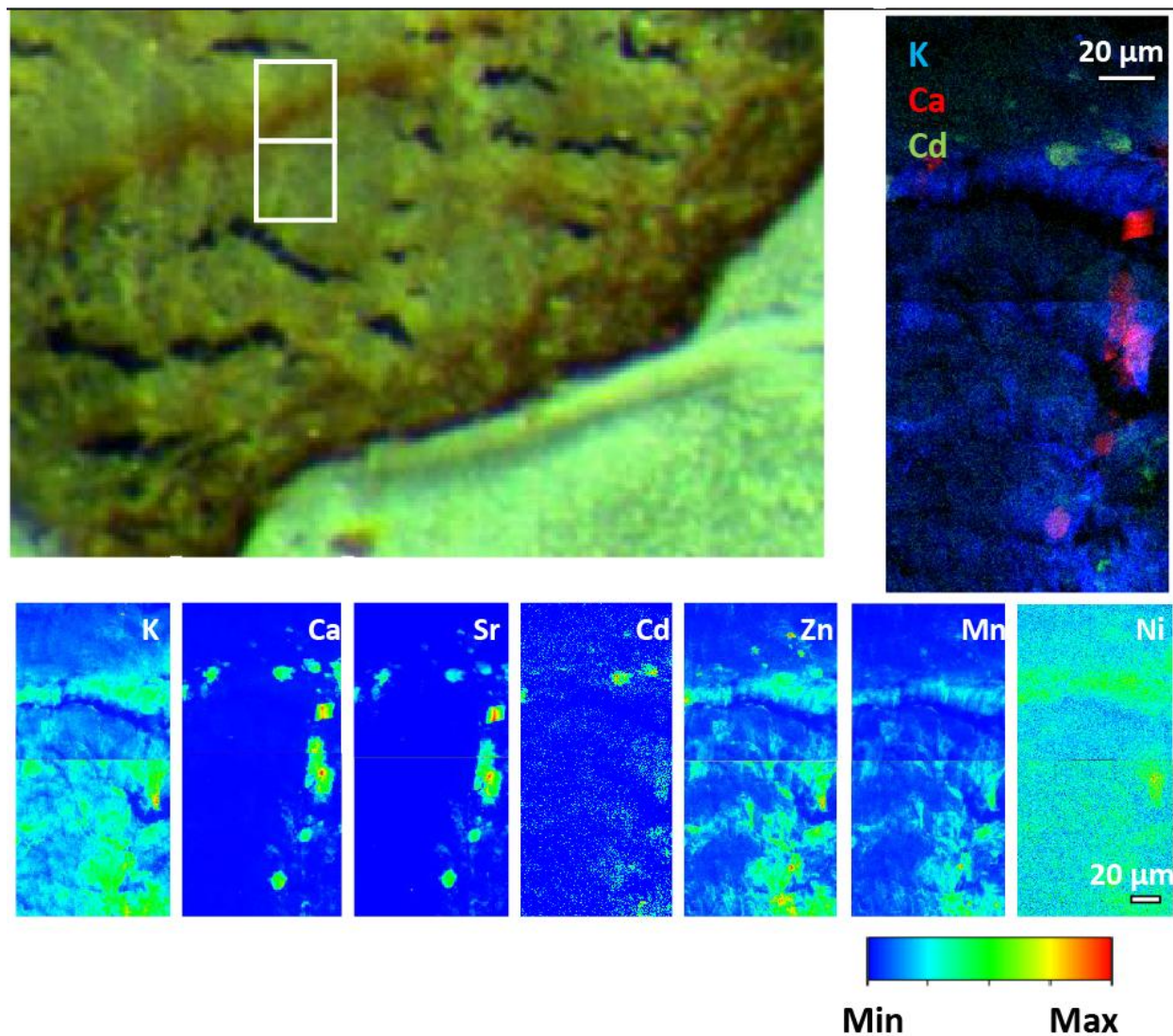


**Figure S5:** Optical image of oven-dried mature branch of biological replicate T4 with the areas analysed with nXRF (rectangles). The RGB image on the right displays the distribution of K (blue), Ca (red), and Cd (green). The heatmaps on the bottom are the nXRF maps of K, Ca, Sr, Cd, Zn, Mn, and Ni. The color scale is adjusted to the range of each element. K was displayed to



show the cellular structure around the cambium. Different forms of Ca-oxalate crystals are observed and in some of them, Cd was included (pixel size 0.1  $\mu\text{m}$ ).

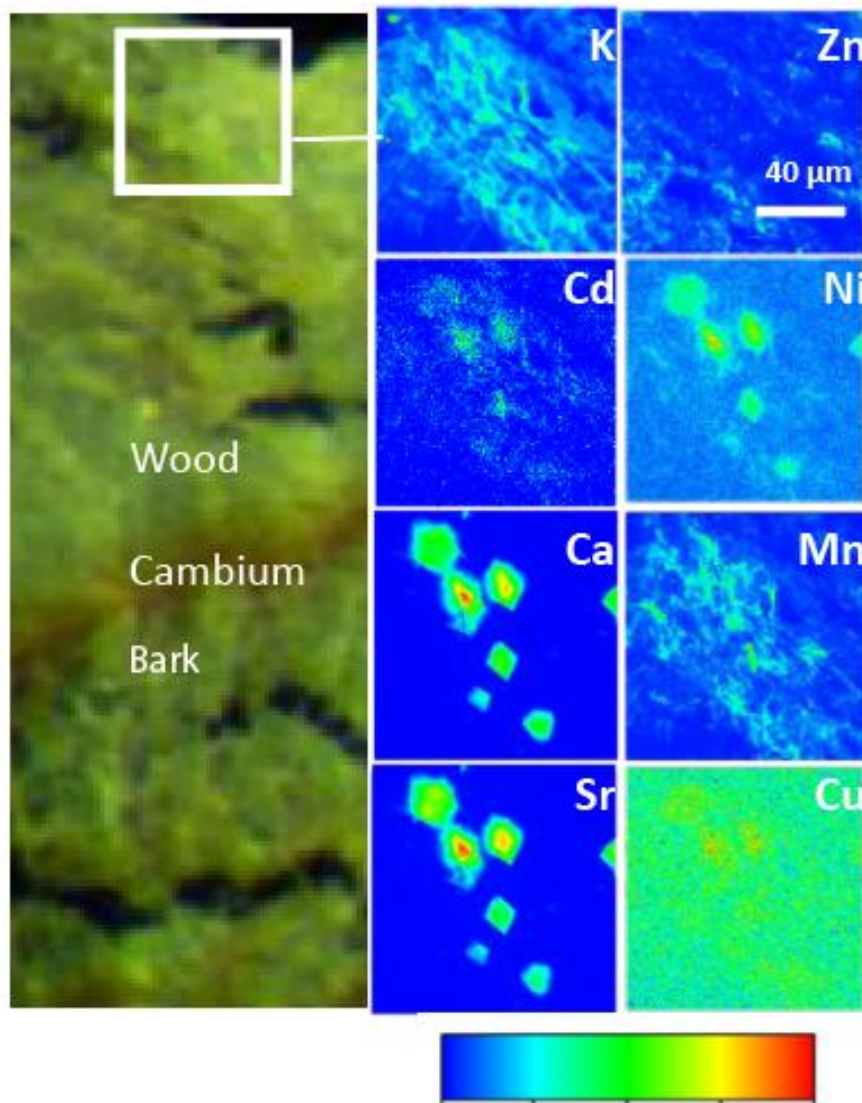


**Figure S6:** Left: Optical image of oven dried mature branch of biological replicate T4 with the areas analysed with nXRF (rectangles). Right: heatmaps with the distribution of K, Zn, Cd, Ni, Ca, Mn, Sr, and Cu in this region. The color scale (blue = minimum and red = maximum photon counts) is adjusted to the range of each element. K was displayed to show the cellular structure



of the periderm area. A group of Ca-oxalate crystals was observed in the wood and, in some, Cd and Ni are included. Zinc and Mn were not observed in these crystals (pixel size 0.1  $\mu\text{m}$ ).

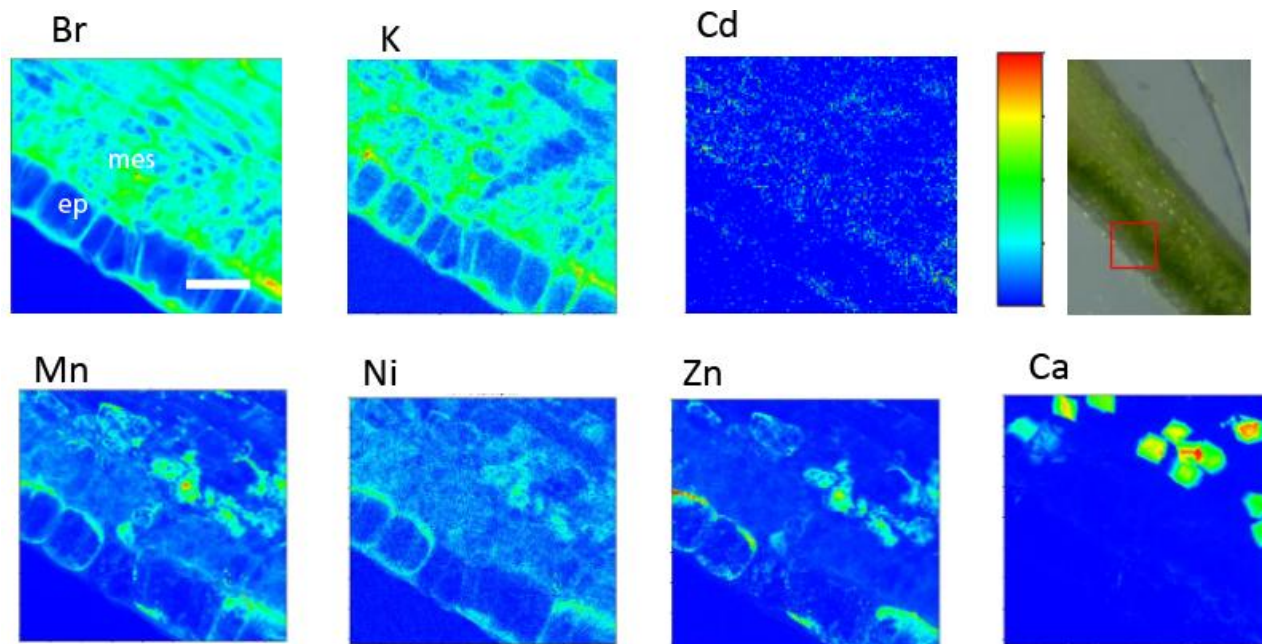


**Figure S7:** Optical image of leaf blade of freeze-dried leaf of biological replicate T6 with the area analyzed with nXRF (upper epidermis region). The heatmaps show the distribution of Br, K, Cd, Mn, Ni, Zn, and Ca (pixel size: 0.1  $\mu\text{m}$ ). The color scale is adjusted to the range of each element.

Cadmium was absent in the epidermis and present in the mesophyll. A cluster of Ca-oxalate crystals were observed in the mesophyll. However, there is no particular incorporation of Mn, Ni, Zn or Cd within these crystals. Scalebar: 20  $\mu\text{m}$ . Ep: epidermis, mes: mesophyll.

### 1.3. References

Castillo-michel, H., Larue, C., Pradas del Real, A., Cotte, M., Sarret, G., 2017. Practical review

on the use of synchrotron based micro- and nano- X-ray fluorescence mapping and X-ray absorption spectroscopy to investigate the interactions between plants and engineered nanomaterials. *Plant Physiol. Biochem.* 110, 13–32.  
<https://doi.org/10.1016/j.plaphy.2016.07.018>

Isaure, M.P., Fayard, B., Sarret, G., Pairis, S., Bourguignon, J., 2006. Localization and chemical forms of cadmium in plant samples by combining analytical electron microscopy and X-ray spectromicroscopy. *Spectrochim. Acta - Part B At. Spectrosc.* 61, 1242–1252.  
<https://doi.org/10.1016/j.sab.2006.10.009>